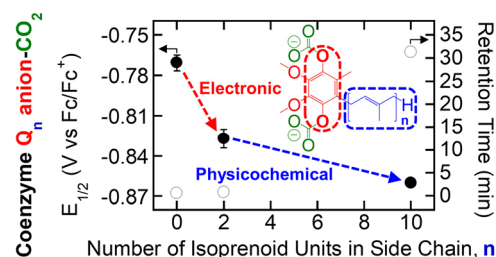


Physicochemical and Electrochemical Investigation of Naturally Occurring Quinones for Application toward Electrochemically Mediated Carbon Dioxide Capture

Kai-Jher Tan, Laura Kuger, Matthias Franzreb, and T. Alan Hatton*

ABSTRACT: The physicochemical and electrochemical characteristics of two naturally occurring quinone families were studied in the context of electrochemical CO₂ capture. Due to their dissimilar lipophilic isoprenoid side chains and quinone redox centers, Vitamin K and Coenzyme Q homologues possess intrinsically adjustable physicochemical properties that were characterized using the Hansen solubility/log *P* lipophilicity parameters, and experimentally quantified using hydrophobic interaction chromatography and viscosity/diffusivity measurements, with an especially large polarity difference noted between Coenzymes Q₁₀ and Q₀. Cyclic voltammetry experiments revealed CO₂-dependent redox behavior that supported the proposed ECEC mechanism for complex formation between electroreduced 1,4-naphthoquinone-/1,4-benzoquinone-derived nucleophiles and the Lewis acidic CO₂, with the Coenzyme Q adducts exhibiting less negative cathodic peak potentials than the parasitic dioxygen/superoxide half-reaction. Further investigation of Coenzyme Q anions suggested that their CO₂ complexation is potentially affected by both electronic and steric/polarity effects via the presence and length of the side chain substituent, respectively. Inspired by the electron transport role of Coenzyme Q₁₀ in mitochondrial membranes, the enhanced lipophilicity of the nonpolar Coenzyme Q₁₀ compared to the chain-less Q₀ was leveraged to facilitate the heterogeneous CO₂-selective electrochemical response of a Coenzyme Q₁₀ composite in aqueous media, thus illustrating the potential of natural/bioinspired compounds for future redox-active applications.



INTRODUCTION

Rising carbon dioxide levels with attendant increasing environmental temperatures pose a great threat to the sustained well-being of the environment and human livelihood.¹ To combat this global warming, various carbon capture and sequestration technologies have emerged, including adsorbent materials,² amine scrubbing,³ carbonate mineralization,^{4–7} and more recently, electrochemical approaches such as electrodialysis/electrodeionization,^{8,9} capacitive methods,^{10,11} fuel cells,^{12,13} electrochemically modulated complexation,^{14–16} pH swing via proton-coupled electron transfer,^{17–23} and direct binding with redox-active Lewis bases.^{24–28}

The application of electrochemistry to carbon dioxide separation has garnered significant interest,^{29–38} and electrochemical processes hold great potential in facilitating amenable energetic requirements, compact designs, and molecular targeting.^{39–42} A quintessential redox-active Lewis base that reacts selectively and reversibly with carbon dioxide is the quinone. As a result, this class of molecules has subsequently been leveraged for carbon dioxide capture via the electrochemically mediated formation of carbonate adducts,^{43–56} with their investigation as a promising set of electrosorbents also encompassing the exploration of a plethora of different quinones through experimental and computational

means.^{57–62} In contrast to the synthetic nature of many of these substituted compounds, some quinones occur naturally in biological processes.⁶³

Two common families of naturally occurring quinones are Vitamin K and Coenzyme Q, with the former arising from animal, plant, and bacterial sources and linked to blood coagulation,⁶⁴ and the latter present in cells/membranes and possessing antioxidant characteristics.⁶⁵ Due to their redox properties,^{66–68} members of these two groups are also components in organism electron transport chains,^{69,70} and their proton-coupled electron transfer capabilities in the Vitamin K and Q cycles^{71,72} can be repurposed for electrochemical complexation with the Lewis acidic carbon dioxide. Following the growing trend of electrochemical materials development inspired by nature,⁷³ the inherently designed ability of these amphipathic vitamin and vitamin-like nutrients to operate in their natural lipophilic membrane environments^{64,70} can generate possibilities for specialized biomimetic

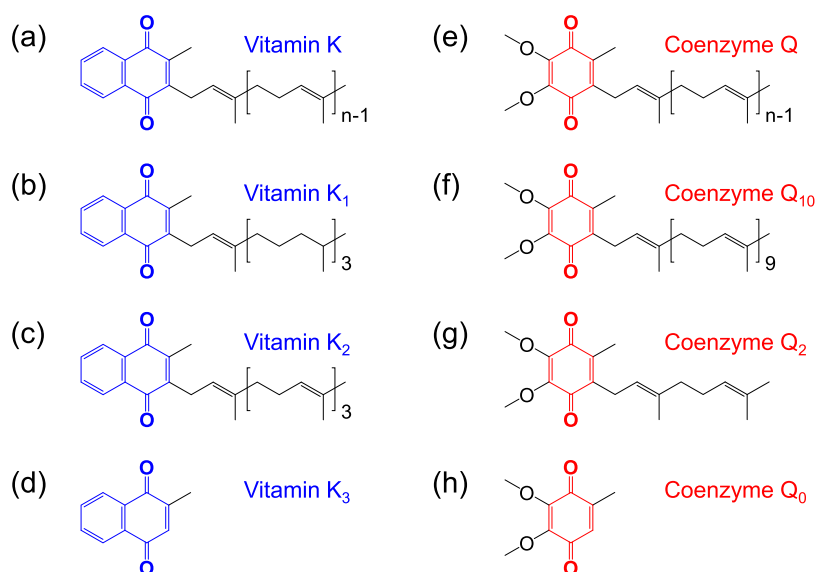


Figure 1. Chemical structures of (a) Vitamin K, (b) Vitamin K₁ (phytonadione), (c) Vitamin K₂ (menaquinone-4), (d) Vitamin K₃ (menadione), (e) Coenzyme Q, (f) Coenzyme Q₁₀ (ubidecarenone), (g) Coenzyme Q₂, and (h) Coenzyme Q₀ (2,3-dimethoxy-5-methyl-1,4-benzoquinone), with their 1,4-naphthoquinone and 1,4-benzoquinone redox-active centers highlighted in blue and red, respectively.

redox-active functionalities in energy applications^{74–76} and sensing.^{77–79} As quinone biological activity is linked with physicochemical properties,⁸⁰ a comprehensive understanding of relevant physicochemical and electrochemical characteristics is thus important in aiding the crossover of these species from biological systems to electrochemically activated carbon capture processes.

In this work, the physicochemical and electrochemical properties of Vitamin K and Coenzyme Q were investigated with regard to their application toward electrochemically mediated carbon dioxide capture. The polarities, viscosities, and diffusivities of several homologues were quantified and analyzed as a function of the length of their isoprenoid side chains using predictive and experimental metrics. Homogeneous electrochemical characterization was performed to analyze the behavior of Vitamin K and Coenzyme Q in the presence of carbon dioxide and to determine the redox potentials of the resulting quinone anion-carbon dioxide adducts relative to the parasitic dioxygen/superoxide reaction. Various Coenzyme Q quinones were further examined in order to explore the influences of the tunable isoprenoid side chain motif. The conductive effect of quinone lipophilicity on their solubilities in aqueous environments mirrored the biological role of Coenzyme Q₁₀ as an electron carrier in the nonpolar mitochondrial membrane and enabled a Coenzyme Q₁₀-containing redox-active interface to interact selectively with carbon dioxide. As such, the results of this work illustrate the potential of applying naturally occurring redox-active quinones with naturally tunable physicochemical properties to electrochemical carbon dioxide capture and provide insight for the use of future bioinspired or synthetic materials to achieve desired functionalities in areas such as molecular targeted separations,^{81–84} sensing and other stimuli-responsive applications,^{83–85} catalysis,^{86,87} and energy storage.

METHODS

All chemicals were obtained from Sigma-Aldrich unless otherwise specified. Vitamin K₁ (BioXtra, ≥99.0%, mixture of isomers), Vitamin K₂ (Menaquinone-4), Vitamin K₃ (crystal-

line), 1,4-naphthoquinone (97%), Coenzyme Q₁₀ (≥98%), Coenzyme Q₄ (≥90%), Coenzyme Q₂ (≥90%), Coenzyme Q₁ (Enzo Life Sciences, Inc., ≥95%), Coenzyme Q₀, 1,4-benzoquinone (reagent grade, ≥98%), nitrogen (in-house supply), and carbon dioxide (Airgas, Bone Dry) were used as received.

Characterization of the Vitamin K and Coenzyme Q species was performed with a variety of methods. Hansen solubility parameters and log *P* octanol–water partition coefficients were determined by using the Molecular Modeling Pro Plus software (Norgwyn Montgomery Software). Isocratic reversed-phase high-performance liquid chromatography (RP-HPLC) was conducted using a 1260 Infinity II LC System (Agilent) equipped with a Poroshell 120 EC-C18 column (Agilent, 4.6 mm × 50 mm, 2.7 μm particle size) and a diode array UV–vis detector, with pure methanol (Optima, Fisher Scientific, LC/MS grade ≥99.9%) as the eluent and analyte solvent. Dynamic viscosities were measured with a microVisc small sample viscometer (RheoSense). Homogeneous cyclic voltammetry was carried out on a VersaSTAT 3 potentiostat (Princeton Applied Research) under quiescent conditions in 5 mL of *N,N*-dimethylformamide (anhydrous, 99.8%) solution with 0.1 M tetrabutylammonium perchlorate (≥99.0%) and 1.1 mM ferrocene (98%) (as an internal standard, if required), using ca. 20 mL cylindrical glass cell vials with a 0.5 mm platinum wire (BASi) as the counter electrode, a silver wire (Premion, Thermo Scientific Chemicals, 0.5 mm diameter, 99.9985% metals basis) as the pseudoreference electrode, and an MF-2012 3.0 mm diameter glassy carbon working electrode (BASi). Nuclear magnetic resonance (NMR) spectroscopy was performed on an Avance NEO 500 MHz NMR spectrometer (Bruker) equipped with a 5 mm Broadband Observation (BBO) Prodigy cryoprobe (Bruker), using samples prepared in CDCl₃ (99.8% D + 0.05% volume basis TMS, Cambridge Isotope Laboratories). Ultraviolet–visible (UV–vis) spectroscopy measurements were completed on a Cary 60 spectrophotometer (Agilent) with a quartz cuvette. Heterogeneous cyclic voltammetry was carried out on a VersaSTAT 3 potentiostat (Princeton Applied Research) under quiescent conditions in

ca. 4 mL aqueous solution saturated with lithium chloride ($\geq 99\%$), using ca. 20 mL cylindrical glass cell vials with a 0.5 mm platinum wire (BASi) as the counter electrode, an RE-5B MF-2052 Ag/AgCl (3 M NaCl) reference electrode (BASi) (aqueous), and a Coenzyme Q_{10} -carbon nanotube (Coenzyme Q_{10} @CNT) working electrode that was prepared by drop-casting a carbon nanotube ($>98\%$, 6–13 nm O.D. \times 2.5–20 μ m L) dispersion onto a piece of conductive carbon cloth (AvCarb 1071 HCB, Fuel Cell Earth) followed by the subsequent drop-casting of a Coenzyme Q_{10} solution onto the carbon nanotube layer after it had dried under ambient conditions. Cyclic voltammetry experiments carried out in the presence of nitrogen and carbon dioxide were achieved by bubbling the solution with the specified gas for at least 20 min and then maintaining a flow of the gas above its surface prior to the electrochemical measurement, unless otherwise specified.

Further details regarding characterization methods can be found in the [Supporting Information](#).

RESULTS AND DISCUSSION

Physicochemical Properties of Vitamin K and Coenzyme Q. The Vitamin K and Coenzyme Q classifications each comprise a variety of compounds that differ in terms of the length and degree of saturation of the hydrophobic and aliphatic isoprenoid side chain connected to their redox-active 1,4-naphthoquinone (NQ) and 1,4-benzoquinone (BQ) centers,^{64,65} respectively, both of which naturally provide a degree of tunability over the physicochemical properties of the overall molecule. The chemical structures of Vitamin K, Vitamin K_1 (phytonadione), Vitamin K_2 (menaquinone-4), Vitamin K_3 (menadione), Coenzyme Q_1 , Coenzyme Q_{10} (ubidecarenone), Coenzyme Q_2 , and Coenzyme Q_0 (2,3-dimethoxy-5-methyl-1,4-benzoquinone) are shown in [Figure 1](#). Vitamin K_1 and Vitamin K_2 possess isoprenoid chains with the same length but different degrees of saturation, and Vitamin K_3 and Coenzyme Q_0 are the chain-less forms of Vitamin K and Coenzyme Q, respectively.

Hansen Solubility Parameters. Differences between the Vitamin K and Coenzyme Q variants were first explored using the Hansen solubility parameters, which were originally proposed for predicting polymer solubility but have since been widely used in other applications.⁸⁸ Each molecule was characterized using the Hansen total solubility parameter, $\delta_{t,X}$ (eq 1):^{88,89}

$$\delta_{t,X}^2 = \delta_{D,X}^2 + \delta_{P,X}^2 + \delta_{H,X}^2 \quad (1)$$

where $\delta_{D,X}/\delta_{P,X}/\delta_{H,X}$ are the dispersion/polar/hydrogen bonding force parameters for species X. It was seen that $\delta_{t,X}$ exhibited a negative correlation with the number of isoprene units present in the side chain for both the 1,4-naphthoquinone and 1,4-benzoquinone derivatives, which suggests that the chain length affects their affinities toward other compounds ([Figure 2a](#)). To investigate this further, the Hansen solubility parameters were extended to the concept of a Hansen distance between species X and a reference solvent j, $R_{X,j}$ (eq 2):^{88,90}

$$R_{X,j}^2 = 4(\delta_{D,X} - \delta_{D,j})^2 + (\delta_{P,X} - \delta_{P,j})^2 + (\delta_{H,X} - \delta_{H,j})^2 \quad (2)$$

where $\delta_{D,j}/\delta_{P,j}/\delta_{H,j}$ are the dispersion/polar/hydrogen bonding force parameters for solvent j. As a higher Hansen distance

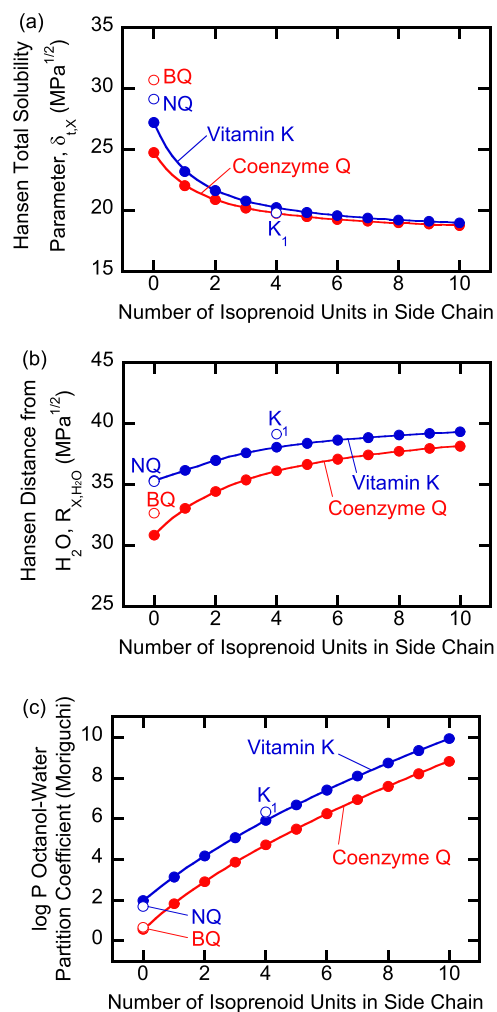


Figure 2. (a) Hansen total solubility parameters, (b) Hansen distances from water, and (c) log *P* octanol–water partition coefficients (calculated using Moriguchi’s method with the Molecular Modeling Pro Plus software) of various Vitamin K and Coenzyme Q quinones vs the number of isoprenoid units present in their side chains.

predicts a lower extent of dissolution, setting water as the reference solvent allows R_{X,H_2O} to serve as an approximate metric for the hydrophobicity of species X. Interestingly, although R_{X,H_2O} rose expectedly with the chain length, the magnitude of its change was dissimilar between Vitamin K and Coenzyme Q ([Figure 2b](#)), in contrast to the relatively uniform trend for $\delta_{t,X}$ across both quinone types. Additionally, the value of R_{X,H_2O} for 1,4-benzoquinone fell between that of Coenzyme Q_0 and Coenzyme Q_1 , despite the fact that 1,4-benzoquinone does not possess a side chain. These observations were noted to be even more prominent with $R_{X,MeOH}$ ([Figure S1](#)), and thus imply that there may be other factors that dictate the behavior of the studied quinones.

log *P* Octanol–Water Partition Coefficients. As the nonpolar characters of Vitamin K and Coenzyme Q originate from unbranched side chains that share a similar structure with the straight chain octanol, their overall lipophilicities were investigated via the log *P* octanol–water partition coefficient (eq 3):⁹¹

$$\log P = \log \frac{[X]_{\text{octanol}}}{[X]_{\text{water}}} \quad (3)$$

where $[X]_{\text{octanol}}$ and $[X]_{\text{water}}$ are the equilibrium concentrations of X in the octanol and water phases, respectively. Like R_{X,H_2O} , values of $\log P$ acquired on a fragment basis,⁹² an atom basis,⁹³ and via Moriguchi's method^{94,95} all increased with the length of the side chain, with those of the 1,4-naphthoquinone compounds being higher than those of their 1,4-benzoquinone complements, and Vitamin K₁ also predicted to be more lipophilic than Vitamin K₂ (Figures 2c and S2). As such, the consistency between the predicted trends of both variables thus further supports the suitability of R_{X,H_2O} for describing the hydrophilicities of Vitamin K and Coenzyme Q.

Experimental Polarities via RP-HPLC. In order to supplement the calculated Hansen and $\log P$ parameters, the polarities of several Vitamin K and Coenzyme Q homologues were assessed experimentally via RP-HPLC with pure methanol as the mobile phase (Figure 3a). As expected, the isoprenoid chain lengths of the tested Coenzyme Q forms were positively and nonlinearly associated with their retention times on a C18 column, revealing a substantial 30.71 min differential between Coenzymes Q₁₀ and Q₀ (Figure 3b) that was in line with previous results obtained using a different mobile phase.⁹⁶ However, the nature of the observed trend deviated starkly from those predicted for the Hansen and $\log P$ parameters (Figures 2, S1, and S2), with the incommensurately large ca. 20-fold jump from 1.39 min (Coenzyme Q₄) to 31.27 min (Coenzyme Q₁₀) highlighting the significant influence of chain length on the nonpolarity of Coenzyme Q. Furthermore, a marked difference was noted between the retention times of Vitamin K₁, Vitamin K₂, and Coenzyme Q₄ at 4.17, 2.31, and 1.39 min, respectively, even though the three compounds share the same 20-carbon chain length. Similarly, but more subtly, the side chain-less Vitamin K₃, 1,4-naphthoquinone, Coenzyme Q₀, and 1,4-benzoquinone exhibited close but non-identical retention times in the range of 0.54–0.62 min. As the aforementioned molecules were characterized using an affinity mechanism based on analyte polarity, these two nontrivial discrepancies likely stemmed from the higher degree of chain saturation in Vitamin K₁ as previously observed,⁹⁷ as well as the presence of other specific substituents bonded to the redox center. Thus, this implies that in addition to the main effect of the isoprenoid chain length on overall molecule retention time, both the chemical structure of the side chain and the composition of the redox-active moiety in the quinones also influence their polarities.

Dynamic Viscosities. Additional experiments were carried out to measure the dynamic viscosities of homogeneous solutions prepared by separately dissolving Vitamin K and Coenzyme Q species in *N,N*-dimethylformamide (Figure 3c). The obtained values were observed to increase with the length of the side chain in a manner similar to the nonlinear relationships previously reported in the literature for hydrocarbons⁹⁸ and polymers,⁹⁹ and also decreased expectedly with an elevation in solution temperature (Table S1). Although the ca. 2-fold larger dynamic viscosity of Coenzyme Q₁₀ relative to the other tested molecules may be less favorable if higher quinone concentrations are required, the 0.7–2.2 mPa·s range of the ca. 50 mM Vitamin K/Coenzyme Q solutions was much lower (ca. an order of magnitude or even more in some cases) than those of the ionic liquids⁴⁹ and liquid quinone-salt-diluent

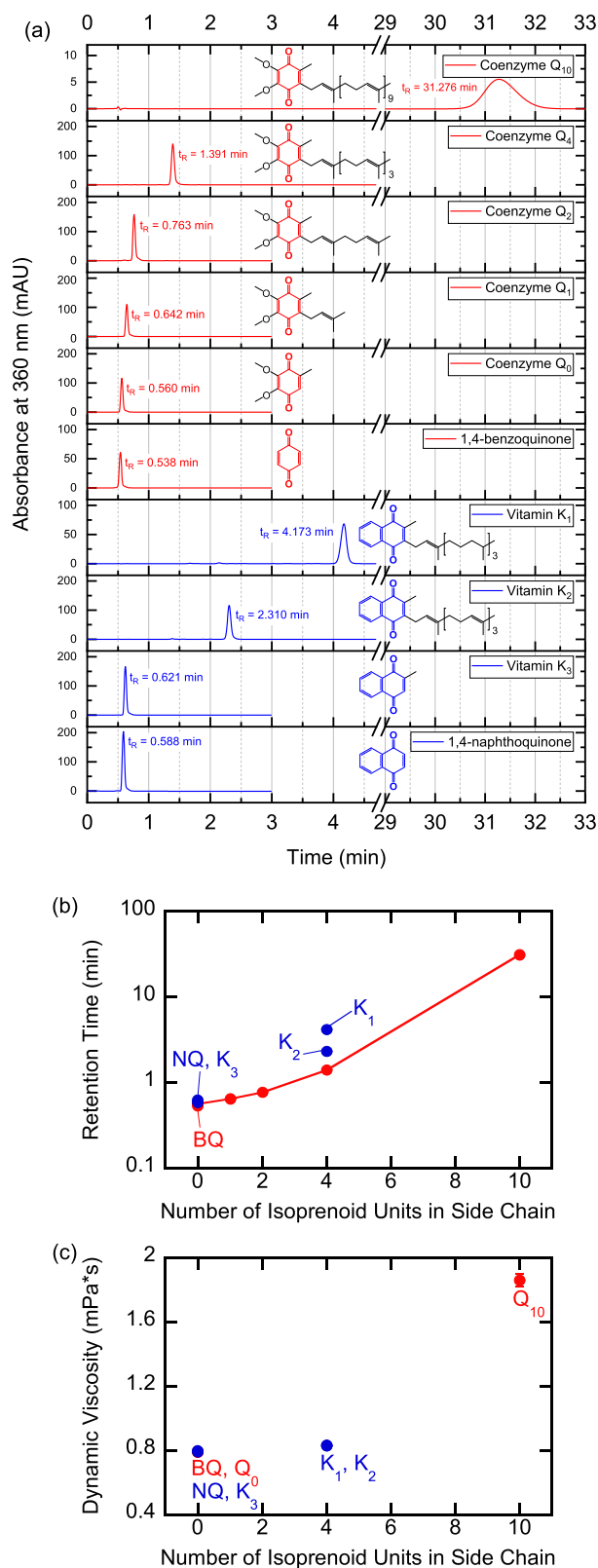


Figure 3. (a) Reversed-phase high-performance liquid chromatograms and their associated (b) retention times (t_R) and (c) dynamic viscosities at 25 °C of various Vitamin K and Coenzyme Q quinones vs the number of isoprenoid units present in their side chains. Results were obtained using a C18 column and pure methanol mobile phase with a 10 nmol quinone loading for (a) and (b), and from *N,N*-dimethylformamide solutions with a ca. 50 mM quinone concentration for (c).

mixtures⁵⁴ previously used for electrochemical carbon dioxide capture in homogeneous environments. As such, the functionality provided by Vitamin K and Coenzyme Q via the adjustable nature of their polarities thus warrants further examination.

Homogeneous Electrochemical Behavior of Vitamin K and Coenzyme Q in an Aprotic Solvent. In order to systematically evaluate the effects of the quinone moiety and the chain length on the resulting electrochemical behavior of the overall redox-active species, 1,4-naphthoquinone- and 1,4-benzoquinone-derived molecules with different aliphatic chain lengths of identical repeating unsaturated isoprene units were selected for homogeneous testing in *N,N*-dimethylformamide.

Electrochemical Behavior in the Presence of Nitrogen and Carbon Dioxide. Cyclic voltammetry experiments were performed in both nitrogen and carbon dioxide environments for Vitamin K₂ ((2-methyl-1,4-naphthoquinone)-(isoprene)₄), Vitamin K₃ ((2-methyl-1,4-naphthoquinone)-(isoprene)₆), Coenzyme Q₁₀ ((2,3-dimethoxy-5-methyl-1,4-benzoquinone)-(isoprene)₁₀), and Coenzyme Q₀ ((2,3-dimethoxy-5-methyl-1,4-benzoquinone)-(isoprene)₀). In aprotic solvents, quinones possess two redox couples corresponding to the following cathodic half-reactions (eqs 4 and 5):¹⁰⁰



where Q is the neutral quinone, $Q^{\cdot -}$ is the semiquinone, and Q^{2-} is the quinone dianion. Under nitrogen gas in *N,N*-dimethylformamide, both events manifested clearly as two sets of well-defined redox signals for all four species (Figure 4a,b). Hydroxylic additives^{58,62,100–104} and the Lewis acidic carbon dioxide^{43–56} have been noted to influence quinone electrochemistry in aprotic media, and in the case of the latter, reduced quinones behave as nucleophiles and have been classified as either “strongly” or “weakly” complexing depending on the proposed order of steps via which they form mono- and diadducts.^{57,105,106} Accordingly, the cyclic voltammograms of Vitamin K₂, Vitamin K₃, Coenzyme Q₁₀, and Coenzyme Q₀ all transitioned from the aforementioned four-peak signal to a two-peak signal in the presence of carbon dioxide gas (Figure 4c,d and S3), with the latter indicative of concerted or closely sequenced electron reductions. Specifically, it has been proposed that this phenomenon is representative of an ECEC (“electrochemical–chemical–electrochemical–chemical”) mechanism whereby the electrochemically generated semiquinone (eq 4) first reacts with a stoichiometric amount of carbon dioxide before further reducing to the dianion form (eq 5) for the capture of an additional carbon dioxide molecule (Figure 5).^{45,57,105,106} The observed merging of the two pairs of peaks into a single pair for Vitamin K and Coenzyme Q is consistent with and suggests the retention of the previously reported “strongly” binding behavior of their corresponding 1,4-naphthoquinone and 1,4-benzoquinone anion redox centers with carbon dioxide,^{46,53,57,105,106} respectively (Figure S4). Upon reintroducing nitrogen into a carbon dioxide-bubbled solution containing Coenzyme Q₁₀, its two original redox couples appeared once again (Figure S5), thus illustrating that the neutral quinone does not react irreversibly with carbon dioxide in the bulk solution.

Redox Potentials Relative to the Dioxygen/Superoxide Redox Couple. In the context of carbon dioxide separation, quinone redox properties are of particular interest and

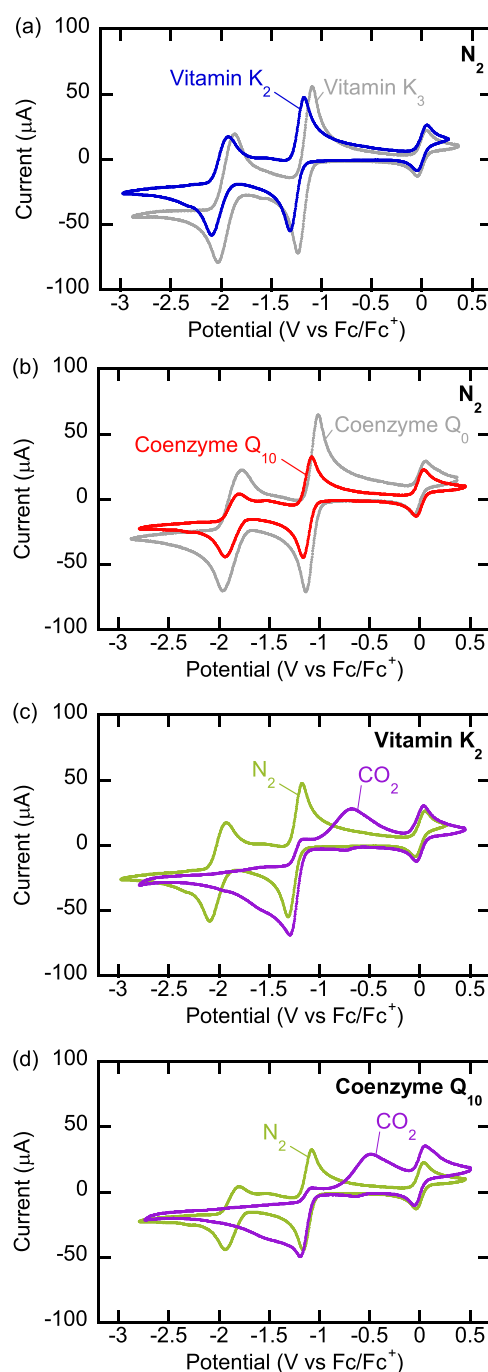


Figure 4. Cyclic voltammograms in *N,N*-dimethylformamide of (a) Vitamin K₂ and Vitamin K₃ under nitrogen, (b) Coenzyme Q₁₀ and Coenzyme Q₀ under nitrogen, (c) Vitamin K₂ under nitrogen and carbon dioxide, and (d) Coenzyme Q₁₀ under nitrogen and carbon dioxide. Results were obtained with 5 mM analyte after five cycles (scanned from 1.25 to −2 V vs Ag wire, followed by a reversal of the scan direction to 1.25 V vs Ag wire for one complete cycle) at 0.05 V/s in 0.1 M NBu₄ClO₄ under each gas and 1.1 mM ferrocene as an internal standard. For (b) and (d), the same solution was run first under nitrogen and then carbon dioxide.

significance due to the occurrence of parasitic dioxygen electroreduction¹⁰⁷ at negative potentials. As oxygen and the formed superoxide species can interact detrimentally with quinone anions^{108,109} as well as carbon dioxide,^{110,111} respectively, it is naturally desirable for quinone anion-carbon dioxide adducts to possess redox potentials more positive than

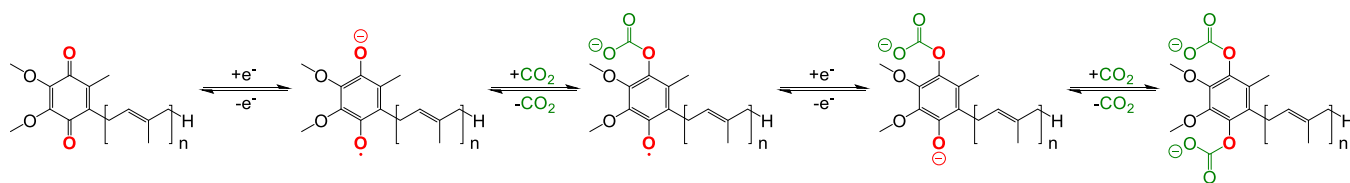


Figure 5. Proposed ECEC mechanism for the formation of Coenzyme Q anion-carbon dioxide adducts that illustrates the “strongly” complexing behavior observed experimentally between Vitamin K/Coenzyme Q anions and carbon dioxide.

that of the $O_2/O_2^{\cdot-}$ couple.⁵⁷ To analyze this further, the halfway potential, $E_{1/2}$ (i.e., the average of the anodic peak potential, E_{ox} , and the cathodic peak potential, E_{red}),¹¹² of each set of redox peaks detected in the presence of either nitrogen or carbon dioxide during cyclic voltammetry was determined experimentally for Vitamin K₂, Vitamin K₃, Coenzyme Q₁₀, Coenzyme Q₀, 1,4-naphthoquinone, and 1,4-benzoquinone (Figure 6a). The resulting values for Vitamin K₂/K₃ and

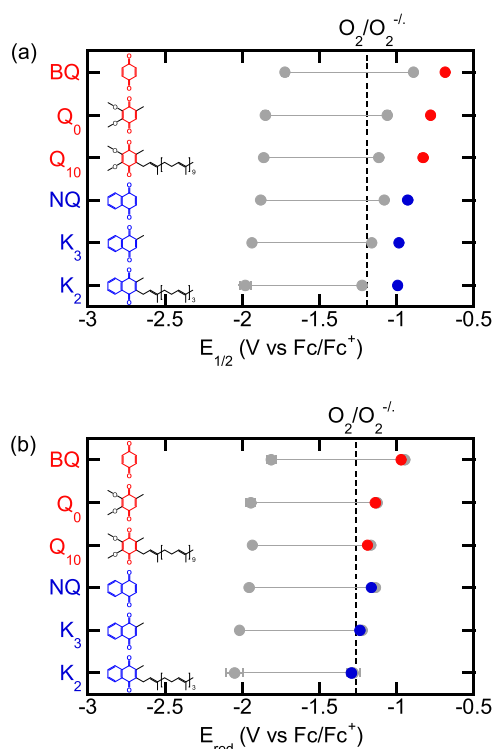


Figure 6. (a) Halfway and (b) cathodic peak potentials of Vitamin K₂, Vitamin K₃, 1,4-naphthoquinone, Coenzyme Q₁₀, Coenzyme Q₀, and 1,4-benzoquinone under nitrogen (gray, with the two points signifying the potentials for the two redox events) and carbon dioxide (red or blue). Results were obtained from cyclic voltammograms with 5 mM analyte after five cycles (scanned from 1.25 to −2 V vs Ag wire, followed by a reversal of the scan direction to 1.25 V vs Ag wire for one complete cycle) at 0.05 V/s in 0.1 M NBu₄ClO₄ *N,N*-dimethylformamide solution under each gas, and 1.1 mM ferrocene as an internal standard. In all cases, the same solution was run first under nitrogen and then carbon dioxide.

Coenzyme Q₁₀/Q₀ were similar to those of their parent 1,4-naphthoquinone and 1,4-benzoquinone molecules, respectively, with the observed trends of 1,4-benzoquinone > Coenzyme Q₀ > Coenzyme Q₁₀, and 1,4-naphthoquinone > Vitamin K₃ > Vitamin K₂ matching previously obtained Hammett substituent constant relationships between the first quinone reduction event halfway potential (eq 4) and the σ_{para}

parameter (Table S2),^{113,114} and ascribed to a general increase in basicity from the number of electron-donating functional groups attached to the quinone redox center.^{47,53,57,59,101,114–119} Under carbon dioxide, not one of the measured $E_{1/2}$ potentials was less than or equal to $E_{1/2}^{O_2/O_2^{\cdot-}}$ (−1.19 V vs Fc/Fc⁺),¹⁰⁷ and those of the 1,4-benzoquinone-containing molecules remained greater than their 1,4-naphthoquinone-containing counterparts. While the halfway potentials of the studied quinone anion-carbon dioxide adducts seem to suggest the suitability of their quinones as carbon dioxide electrosorbents, additional cathodic overpotentials from kinetic or mass transfer limitations may need to be overcome in order for complexation to be achieved, and as such, the cathodic peak potential, E_{red} , was employed⁵⁷ to more stringently characterize the previously observed redox events (Figure 6b). Compared to $E_{1/2}$, the E_{red} potentials of the carbon dioxide complexes were expectedly much closer to that of molecular oxygen reduction, with the E_{red} of Vitamin K₂ observed to be more negative than $E_{red}^{O_2/O_2^{\cdot-}}$ (−1.27 V vs Fc/Fc⁺).¹⁰⁷ Contrastingly, both Coenzyme Q₀ and Coenzyme Q₁₀ exhibited E_{red} values above $E_{red}^{O_2/O_2^{\cdot-}}$, and as such, the properties of Coenzyme Q were subject to additional investigation. It is interesting to note that although Coenzyme Q₀ and short-chain Coenzyme Q homologues have been reported to react with superoxide to yield reduced semiquinones,^{108,109} Coenzyme Q₁₀ appeared to either stabilize or be in close proximity to the $O_2^{\cdot-}$ radicals,¹⁰⁹ which suggests a potential benefit to the presence of its long side chain.

Effect of Side Chain on Coenzyme Q Properties. In an effort to better understand the extent of electronic and other effects on the electrochemical behavior of Coenzyme Q, the variation in its properties with chain length was probed using Coenzyme Q₁₀, Coenzyme Q₂, and Coenzyme Q₀.

Redox Potentials of Coenzyme Q Anion-Carbon Dioxide Adducts. The $E_{1/2}$ of Coenzyme Q₀ under carbon dioxide was previously observed to be less negative than that of Coenzyme Q₁₀ (Figure 6a), which was attributed to the heightened basicity of Coenzyme Q₁₀ due to its additional side chain group. As such, the redox potential of Coenzyme Q₂ relative to Coenzyme Q₁₀ is of interest, as the two quinones possess the same substituent, with the only difference being the number of isoprene units present in each. Although both the halfway and cathodic peak potentials of the three Coenzyme Q variants were seen to be more positive than those of $O_2/O_2^{\cdot-}$ (Figure S6), the halfway potential framework was selected in this case for tracking the peaks obtained from cyclic voltammetry in order to provide a better estimate of the standard potential as a thermodynamic property. Interestingly, the $E_{1/2}$ of the Coenzyme Q₂ anion-CO₂ adduct at −0.83 V vs Fc/Fc⁺ was found to lie between those of the Coenzyme Q₀ and Coenzyme Q₁₀ anion-CO₂ adducts at −0.77 and −0.86 V vs Fc/Fc⁺, respectively (Figure 7a). Since the polarities of

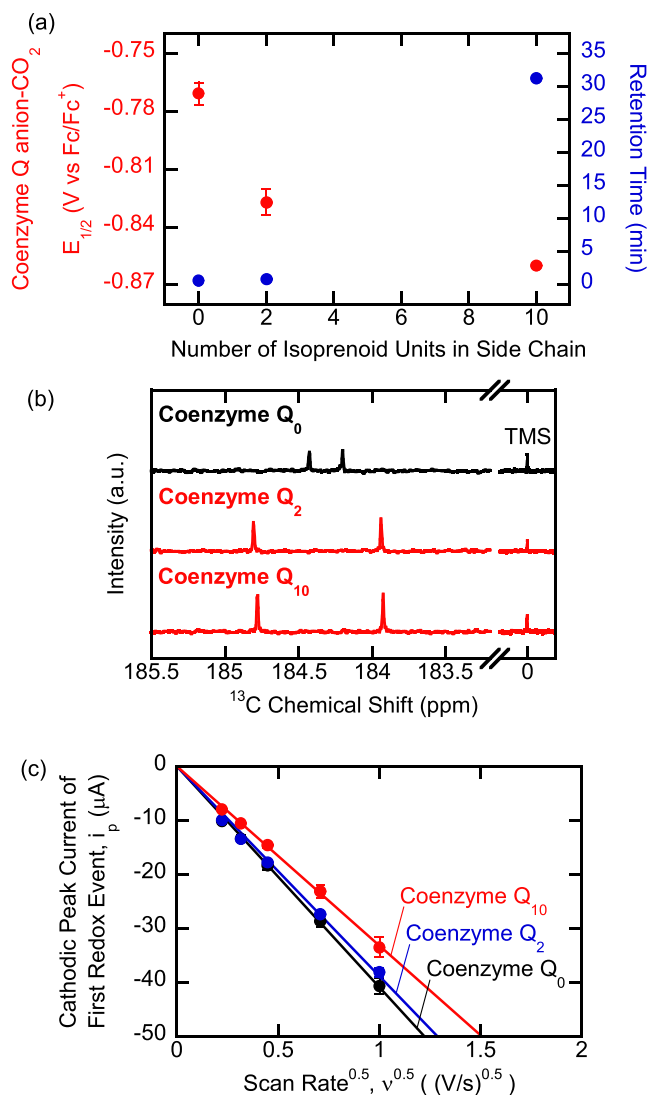


Figure 7. (a) Halfway potentials under carbon dioxide, (b) carbonyl carbon ¹³C nuclear magnetic resonance spectra, and (c) Randles–Sevcik plots under nitrogen for Coenzyme Q₁₀, Coenzyme Q₂, and Coenzyme Q₀. Results in (a) and (c) were obtained from cyclic voltammograms with ca. 1 mM analyte after five cycles (scanned from 1.25 to −2 V vs Ag wire, followed by a reversal of the scan direction to 1.25 V vs Ag wire for one complete cycle) at 0.05 V/s for (a), and two cycles (scanned from 0.5 to −2 V vs Ag wire, followed by a reversal of the scan direction to 0.5 V vs Ag wire for one complete cycle) at each scan rate for (c) in 0.1 M NBu₄ClO₄ N,N-dimethylformamide solution, and 1.1 mM ferrocene as an internal standard in the case of (a). For (a), the same solution was bubbled first with nitrogen for at least 10 min and then with carbon dioxide for at least 20 min, followed by gas flow above its surface before the electrochemical experiment was performed. For (b), solutions were prepared at a concentration of ca. 40 mM quinone in TMS-containing CDCl₃.

Coenzymes Q₀ and Q₂ described by their RP-HPLC retention times (Figure 3a,b) were very similar (0.56–0.76 min) compared to the significantly larger value of Coenzyme Q₁₀ (31.27 min), it is hypothesized that the differences in the $E_{1/2}$ values of the Coenzyme Q₀ and Coenzyme Q₂ anion-CO₂ adducts are predominantly electronic in nature, and the differences in the $E_{1/2}$ values of Coenzyme Q₂ and Coenzyme Q₁₀ in the presence of CO₂ arise from the influence of the side chain length on Coenzyme Q anion-CO₂ adduct formation.

Previous literature has indicated that the redox potential of Coenzyme Q is affected by the orientation of its dimethoxy groups^{120,121} and the rigid/flexible nature of its side chain,¹¹⁷ and that its biological transfer activity changes through variation of its side chain characteristics.¹²²

Carbonyl Carbon ¹³C NMR Chemical Shifts of Coenzyme Q. As a complement to the electrochemical characterization, ¹³C nuclear magnetic resonance spectroscopy was also performed on Coenzyme Q to track the tetramethylsilane (TMS)-referenced chemical shifts of the carbonyl carbons bonded to the redox-active oxygen centers for the intended purpose of revealing any potential electron density changes arising from the absence or presence of its side chain substituent. Two individual signals were detected for each quinone, with those of Coenzymes Q₂ and Q₁₀ sharing the same chemical shifts at 184.8 and 183.9 ppm, but differing slightly from those of Coenzyme Q₀ at 184.4 and 184.2 ppm (Figure 7b), thus implying that the aforementioned observed variations in redox potential of side chain-possessing Coenzyme Q anion-CO₂ adducts may result from chain length-influenced steric or polarity effects rather than the inherent electronic ones seen between the anions of the side chain-less Coenzyme Q₀ and the side chain-bearing Coenzyme Q₂ in the presence of CO₂. In this way, the isoprenoid side chain can serve as a unique tool for unconventionally tuning redox potentials through physicochemical means compared with the more traditional approach of directly adjusting electron density via targeted substituent addition. A similar effect has been observed with self-assembled monolayers composed of ferrocene-terminated straight chain alkanes and coadsorbed alkanethiols, for which an increase in the chain length of the nonpolar coadsorbates shifted the potentials of the redox-active units to more positive values, and was ascribed to a stronger stabilization of ferrocene in the more alkane-like environment.^{123,124} Additionally, steric hindrance has previously been proposed to influence interactions between quinone anions and carbon dioxide,^{59,60,105} and the formation of monocarbonate instead of dicarbonate adducts between tetrahalogenated quinone anions and carbon dioxide has been suggested to be affected by an increased difficulty of the latter in accessing the carbonyl oxygens due to the bulky substituents.¹⁰⁵

Diffusivities of Coenzyme Q. As the ability of a solute to diffuse in an electrolyte medium is relevant to homogeneous electrochemical applications, the diffusivities of Coenzymes Q₁₀, Q₂, and Q₀ were also evaluated via successive cyclic voltammetry conducted with varying scan rates. Specifically, the first reduction event observed in the cyclic voltammograms corresponding to semiquinone generation (eq 4) was used to estimate the apparent diffusion coefficient,^{125,126} D , of the quinone by fitting its experimentally determined cathodic peak currents at different scan rates to the Randles–Sevcik equation (eq 6):¹²⁷

$$i_p = 0.4463AC_o^* \left(\frac{n_{\text{elec}}^3 F^3 D}{RT} \right)^{1/2} \nu^{1/2} \quad (6)$$

where i_p is the peak current, A is the surface area of the electrode, C_o^* is the concentration of the quinone in solution, n_{elec} is the number of electrons transferred in the redox reaction, F is Faraday's constant, ν is the scan rate, R is the gas constant, and T is the temperature. This technique was selected over the pulsed-field gradient nuclear magnetic

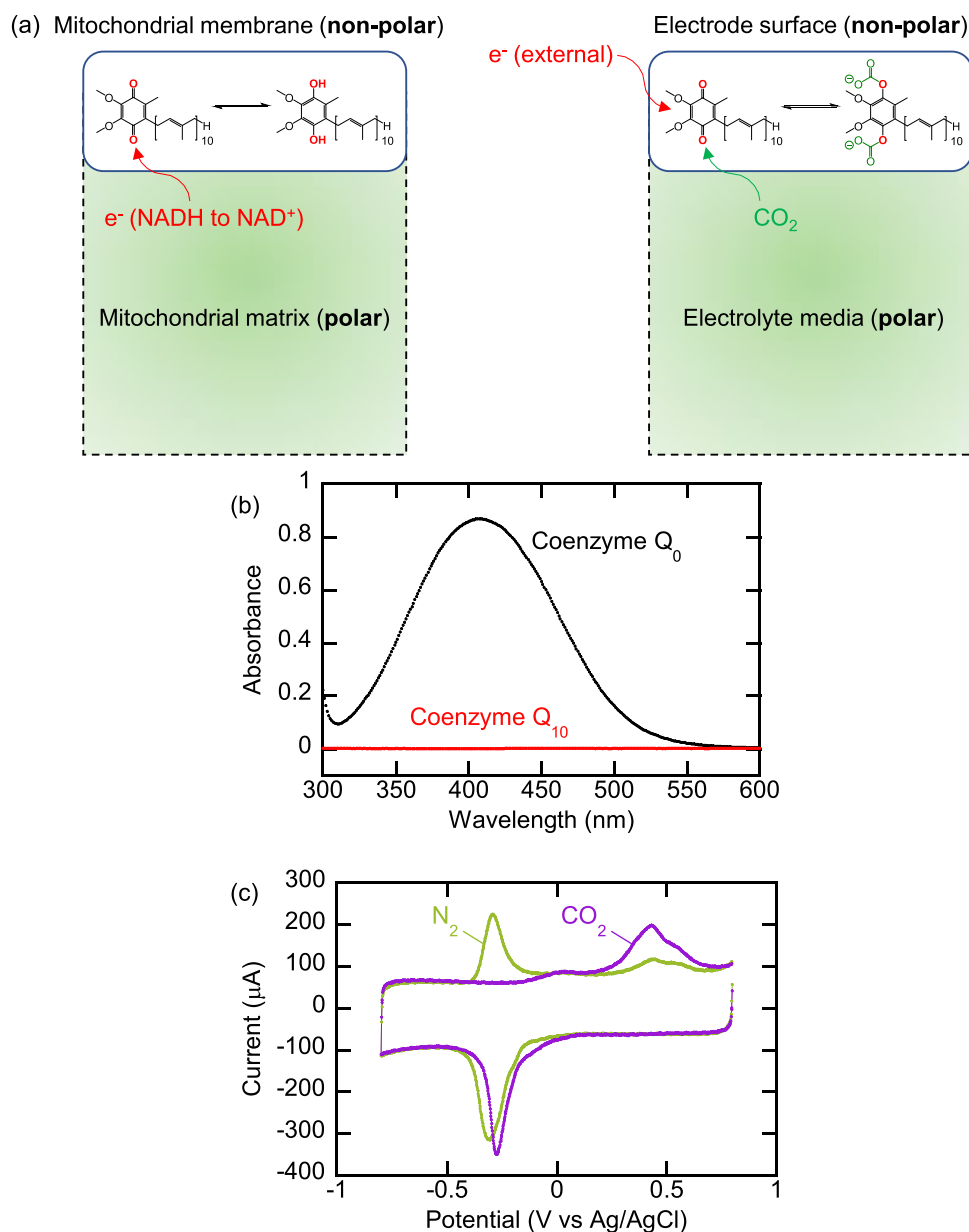


Figure 8. (a) Schematics depicting the interfacial function of Coenzyme Q_{10} in biological processes such as the first step of the mitochondrial electron transport chain (left), and proposed electrochemical processes such as electrochemically mediated carbon dioxide separation (right). (b) UV-vis spectra of water containing ca. $2 \mu\text{mol}$ of Coenzyme Q_{10} (red) and Coenzyme Q_0 (black) per mL after being passed through $0.22 \mu\text{m}$ syringe filters and diluted twofold, and (c) cyclic voltammograms in water saturated with lithium chloride of Coenzyme Q_{10} @CNT under nitrogen and carbon dioxide. For (c), results were obtained after five cycles (scanned from open circuit voltage to 0.8 V vs Ag/AgCl for the zeroth cycle, followed by a reversal of the scan direction to -0.8 V vs Ag/AgCl and finally to 0.8 V vs Ag/AgCl for one complete cycle) at 0.1 V/s under each gas with the same solution run first under nitrogen and then carbon dioxide, and the solution was bubbled with nitrogen/carbon dioxide for at least 10 min, followed by gas flow above its surface before the electrochemical experiment was performed.

resonance spectroscopy method due to its assessment of diffusion in the boundary layer at an electrode surface as opposed to self-diffusion in the bulk phase,¹²⁸ and is thus more pertinent in the context of the electrochemically mediated formation of quinone anion-carbon dioxide adducts. The apparent diffusion coefficients of Coenzyme Q_{10} , Coenzyme Q_2 , and Coenzyme Q_0 were subsequently determined to be 3 , 4 , and $5 \times 10^{-10} \text{ m}^2/\text{s}$, respectively, and appeared to correlate with the number of isoprenoid units in the Coenzyme Q side chain, with the linear relationships between the cathodic peak current and square root of the scan rate (Figure 7c) matching previous electrochemical studies of other Coenzyme Q

derivatives.¹¹⁷ As the calculated values were of the same order of magnitude and noted to be very similar to those of the side chain-free 1,4-benzoquinone, 1,4-naphthoquinone, and 9,10-anthraquinone from the literature,¹²⁹ there does not seem to be a significant drawback with the use of the longer Coenzyme Q_{10} in terms of diffusivity.

Heterogeneous Electrochemical Activation of Coenzyme Q_{10} . In addition to studying the homogeneous behavior of Coenzyme Q , the investigation of its heterogeneous operation as a redox-active interface is also of value in establishing and providing insight with regard to an alternative

potential configuration for electrochemical carbon dioxide separation.

Biomimetic Coenzyme Q_{10} Interface for Electrochemical Carbon Dioxide Adduct Formation. The especially notable difference in polarity between Coenzyme Q_{10} and Coenzyme Q_0 afforded by the length of their side chains and previously observed through RP-HPLC (Figure 3a,b) naturally suggests that a polar environment would be suitable for the heterogeneous activation of the lipophilic Coenzyme Q_{10} due to its inclination to be strongly adsorbed at an electrode interface. In fact, such an arrangement draws inspiration from the first step of the naturally occurring mitochondrial electron transport chain, during which the reduction of Coenzyme Q_{10} in the nonpolar inner mitochondrial membrane with electrons released from the oxidation of reduced nicotinamide adenine dinucleotide (NADH) in the polar mitochondrial matrix is catalyzed by a reductase enzyme.^{130–132} This interfacial redox-active biological process can be analogously transferred to a heterogeneous electrochemical framework (Figure 8a), with two key differences being the direct reduction of Coenzyme Q_{10} with electrons from an external power source instead of NADH and the reaction of the Coenzyme Q_{10} anions with carbon dioxide instead of protons.

Electrochemical Solvent Selection. For the purpose of determining a suitable polar environment, four common electrochemical solvents (water, methanol, acetonitrile, and dimethyl sulfoxide) were screened in terms of properties pertinent to solvent suitability for electrochemical carbon dioxide separation (Table S3). Like their *N,N*-dimethylformamide counterpart used for homogeneous electrochemical characterization, the higher relative permittivities¹³³ and boiling points¹³³ of water and dimethyl sulfoxide were deemed desirable due to their enhanced ease of polarization for electrochemical processes and lower volatilities for reduced solvent loss²⁹ from carbon dioxide mass transfer to the liquid phase via gas sparging, respectively. While water is an attractive solvent with regard to safety, cost efficiency, and natural abundance,^{51,134} its protic nature enables pH changes that affect carbon dioxide dissolution and speciation, as well as quinone reduction,^{100,115,135–140} all of which can then consequently interfere with quinone anion-carbon dioxide adduct formation. As such, in order to minimize any convoluting pH-swing effects and maintain the advantages of an aqueous medium, a saturated lithium chloride water-in-salt formulation was employed to significantly reduce the amount of free water in the solution. The high solubility of lithium chloride (ca. 2.8 mol $H_2O/mol Li^+$) renders it a suitable analogue of lithium bis(trifluoromethanesulfonyl)imide (LiTFSI),¹⁴¹ the latter of which has previously been used as a superconcentrated electrolyte that significantly extends the aqueous electrochemical stability window by suppressing parasitic water splitting reactions, exhibits higher resistance to evaporative losses, and stabilizes the quinone anion-carbon dioxide adduct at higher lithium molalities.^{51,142} Compared to LiTFSI salt-in-water concentrations below 5 molal, the drastically lower water-to-salt ratio for LiTFSI water-in-salt concentrations above 20 molal has been reported to result in both a lower fraction of free water molecules that are not bound to any Li^+ cations, as well as a stronger interaction between the Li^+ and TFSI[−] ions, with the primary solvation sheath of each Li^+ cation possessing fewer water molecules and more TFSI[−] anions.¹⁴² Solubility experiments of Coenzyme Q in water revealed negligible and full dissolution of Coenzyme

Q_{10} and Coenzyme Q_0 , respectively, as evidenced by visual inspection and UV–vis spectroscopy (Figures 8b and S7). Furthermore, these observations corresponded well with the Coenzyme Q–water Hansen distances, R_{Q,H_2O} , calculated using eq 2, which predict a lower propensity of Coenzyme Q_{10} to dissolve in water compared to Coenzyme Q_0 as a result of R_{Q_{10},H_2O} being noticeably greater than R_{Q_0,H_2O} (Table S3), thus illustrating the utility and versatility of the side chain motif. Although the Coenzyme Q–dimethyl sulfoxide pairing also yielded the same trends in dissolution and Hansen distances (Table S3), it was noted that Coenzyme Q_{10} was highly dispersible and slightly soluble in the dimethyl sulfoxide environment (Figures S8 and S9). As such, the aforementioned results thus precluded the need for electrochemical tests involving Coenzyme Q_0 and dimethyl sulfoxide.

Heterogeneous Electrochemical Response of Coenzyme Q_{10} to Nitrogen and Carbon Dioxide in Water-in-Salt Media. As a proof-of-concept, Coenzyme Q_{10} was deposited on a conductive carbon nanotube (CNT) layer to yield a heterogeneous Coenzyme $Q_{10}@CNT$ interface for electrochemical activation. The presence of Coenzyme Q_{10} in the Coenzyme $Q_{10}@CNT$ electrode was evident based on the single set of oxidation and reduction peaks observed from cyclic voltammetry in saturated lithium chloride solution. Accordingly, quinones are expected to undergo an overall two-electron reduction in aqueous media that is facilitated by proton transfer and/or hydrogen bonding,^{100,102} as opposed to the two sequential one-electron reductions previously observed in the aprotic *N,N*-dimethylformamide under nitrogen. Upon electrochemically cycling Coenzyme $Q_{10}@CNT$ in the presence of nitrogen followed by carbon dioxide, a prominent shift in the anodic peak signal of the cyclic voltammogram to more positive potentials was noted (Figure 8c), with the resulting reduced ease of oxidation suggesting preferential quinone anion-carbon dioxide adduct formation and matching previous studies of selective interactions between quinone anions and carbon dioxide in lithium-based water-in-salt media.⁵¹ In this way, the Coenzyme $Q_{10}@CNT$ interface illustrates that the electron-accepting and lipophilic properties of Coenzyme Q can be repurposed and extended to heterogeneous carbon dioxide binding. These results also support that the hydrophobicity and high molecular weight of Coenzyme Q_{10} innately facilitate its heterogeneous functionalization at or in solid electrode surfaces,^{143,144} self-assembled monolayers,^{145,146} phospholipid membranes,^{147,148} and carbonaceous scaffolds,^{149,150} in contrast to other more conventional approaches such as polymerization or covalent bonding that may require further chemical design.


CONCLUSIONS

A variety of Vitamin K and Coenzyme Q homologues were explored for relevance to electrochemical carbon dioxide separation in terms of their physicochemical and electrochemical behavior. The isoprenoid side chain of these compounds provided an innate method for tuning their physicochemical properties, which were subsequently assessed through Hansen solubility and log *P* lipophilicity parameters, RP-HPLC, and viscosity and diffusivity measurements. In the presence of carbon dioxide, the electrochemical responses of Vitamin K and Coenzyme Q supported a previously reported ECEC reaction mechanism, with Coenzyme Q further displaying desirable cathodic peak potentials that were more


positive than that of the parasitic oxygen reduction reaction to superoxide. Additional investigation of several Coenzyme Q variants suggested that the presence and length of their side chains may affect Coenzyme Q anion-CO₂ adduct formation via electronic and steric/polarity effects, respectively. Lastly, the lipophilicity of Coenzyme Q₁₀ was leveraged for its use as a biomimetic interface for electrochemical interaction with carbon dioxide in aqueous media as Coenzyme Q₁₀@CNT, which illustrated its inherent advantage over the water-soluble Coenzyme Q₀ in a heterogeneous configuration. The ability of the naturally occurring Vitamin K and Coenzyme Q quinone families to manifest the influence of both physicochemical and redox-active properties within a single molecule may offer useful insight for the future application of naturally occurring or nature-inspired species in the electrochemical separation of carbon dioxide and/or other analytes, with potential extension to other fields such as catalysis, sensing, and energy storage.


AUTHOR INFORMATION


Corresponding Author

T. Alan Hatton – Department of Chemical Engineering, Massachusetts Institute of Technology, Cambridge, Massachusetts 02139, United States;  orcid.org/0000-0002-4558-245X; Email: tahatton@mit.edu

Authors

Kai-Jher Tan – Department of Chemical Engineering, Massachusetts Institute of Technology, Cambridge, Massachusetts 02139, United States;  orcid.org/0000-0001-7705-3774

Laura Kuger – Department of Chemical Engineering, Massachusetts Institute of Technology, Cambridge, Massachusetts 02139, United States; Present Address: Institute of Functional Interfaces (IFG), Karlsruhe Institute of Technology, 76344 Eggenstein-Leopoldshafen, Germany;  orcid.org/0000-0001-7323-1158

Matthias Franzreb – Institute of Functional Interfaces (IFG), Karlsruhe Institute of Technology, 76344 Eggenstein-Leopoldshafen, Germany;  orcid.org/0000-0003-3586-4215

Author Contributions

K.-J.T. and T.A.H. conceived the project concept, with significant scientific contributions from L.K. K.-J.T., L.K., and T.A.H. were involved in all scientific considerations. K.-J.T. wrote the manuscript, with revisions and discussions from L.K., M.F., and T.A.H. K.-J.T. and L.K. performed the experiments.

Notes

The authors declare no competing financial interest.

ACKNOWLEDGMENTS

This work made use of the Department of Chemistry Instrumentation Facility (DCIF) at the Massachusetts Institute of Technology. K.-J.T. and T.A.H. acknowledge support from the National Science Foundation (Grant Number 2029442). L.K. was funded by the Karlsruhe House of Young Scientists (KHYS).

ABBREVIATIONS

NQ, 1,4-naphthoquinone; BQ, 1,4-benzoquinone; RP-HPLC, reversed-phase high-performance liquid chromatography; ECEC, electrochemical–chemical–electrochemical–chemical; CNT, carbon nanotube

REFERENCES

- (1) Solomon, S.; Plattner, G.-K.; Knutti, R.; Friedlingstein, P. Irreversible climate change due to carbon dioxide emissions. *Proc. Natl. Acad. Sci. U.S.A.* **2009**, *106* (6), 1704–1709.
- (2) Choi, S.; Drese, J. H.; Jones, C. W. Adsorbent Materials for Carbon Dioxide Capture from Large Anthropogenic Point Sources. *ChemSusChem* **2009**, *2* (9), 796–854.
- (3) Rochelle, G. T. Amine Scrubbing for CO₂ Capture. *Science* **2009**, *325* (5948), 1652–1654.
- (4) Harada, T.; Simeon, F.; Hamad, E. Z.; Hatton, T. A. Alkali Metal Nitrate-Promoted High-Capacity MgO Adsorbents for Regenerable CO₂ Capture at Moderate Temperatures. *Chem. Mater.* **2015**, *27* (6), 1943–1949.
- (5) Matter, J. M.; Stute, M.; Snæbjörnsdóttir, S. Ó.; Oelkers, E. H.; Gislason, S. R.; Aradóttir, E. S.; Sigfusson, B.; Gunnarsson, I.; Sigurdardóttir, H.; Gunnlaugsson, E.; et al. Rapid carbon mineralization for permanent disposal of anthropogenic carbon dioxide emissions. *Science* **2016**, *352* (6291), 1312–1314.
- (6) Keith, D. W.; Holmes, G.; St Angelo, D.; Heidel, K. A Process for Capturing CO₂ from the Atmosphere. *Joule* **2018**, *2* (8), 1573–1594.
- (7) Harada, T.; Halliday, C.; Jamal, A.; Hatton, T. A. Molten ionic oxides for CO₂ capture at medium to high temperatures. *J. Mater. Chem. A* **2019**, *7* (38), 21827–21834.
- (8) Eisaman, M. D.; Alvarado, L.; Larner, D.; Wang, P.; Garg, B.; Littau, K. A. CO₂ separation using bipolar membrane electrodialysis. *Energy Environ. Sci.* **2011**, *4* (4), 1319–1328.
- (9) Datta, S.; Henry, M. P.; Lin, Y. J.; Fracaro, A. T.; Millard, C. S.; Snyder, S. W.; Stiles, R. L.; Shah, J.; Yuan, J.; Wesoloski, L.; et al. Electrochemical CO₂ Capture Using Resin-Wafer Electrodeionization. *Ind. Eng. Chem. Res.* **2013**, *52* (43), 15177–15186.
- (10) Kokoszka, B.; Jarrar, N. K.; Liu, C.; Moore, D. T.; Landskron, K. Supercapacitive Swing Adsorption of Carbon Dioxide. *Angew. Chem., Int. Ed.* **2014**, *53* (14), 3698–3701.
- (11) Legrand, L.; Schaetzle, O.; de Kler, R. C. F.; Hamelers, H. V. M. Solvent-Free CO₂ Capture Using Membrane Capacitive Deionization. *Environ. Sci. Technol.* **2018**, *52* (16), 9478–9485.
- (12) Abdelkareem, M. A.; Lootah, M. A.; Sayed, E. T.; Wilberforce, T.; Alawadhi, H.; Yousef, B. A. A.; Olabi, A. G. Fuel cells for carbon capture applications. *Sci. Total Environ.* **2021**, *769*, No. 144243.
- (13) Muroyama, A. P.; Beard, A.; Pribyl-Kranewitter, B.; Gubler, L. Separation of CO₂ from Dilute Gas Streams Using a Membrane Electrochemical Cell. *ACS ES&T Eng.* **2021**, *1* (5), 905–916.
- (14) Appel, A. M.; Newell, R.; DuBois, D. L.; Rakowski DuBois, M. Concentration of Carbon Dioxide by Electrochemically Modulated Complexation with a Binuclear Copper Complex. *Inorg. Chem.* **2005**, *44* (9), 3046–3056.
- (15) Stern, M. C.; Simeon, F.; Herzog, H.; Hatton, T. A. Post-combustion carbon dioxide capture using electrochemically mediated amine regeneration. *Energy Environ. Sci.* **2013**, *6* (8), 2505–2517.
- (16) Wang, M.; Herzog, H. J.; Hatton, T. A. CO₂ Capture Using Electrochemically Mediated Amine Regeneration. *Ind. Eng. Chem. Res.* **2020**, *59* (15), 7087–7096.

- (17) Watkins, J. D.; Siefert, N. S.; Zhou, X.; Myers, C. R.; Kitchin, J. R.; Hopkinson, D. P.; Nulwala, H. B. Redox-Mediated Separation of Carbon Dioxide from Flue Gas. *Energy Fuels* **2015**, 29 (11), 7508–7515.
- (18) Huang, C.; Liu, C.; Wu, K.; Yue, H.; Tang, S.; Lu, H.; Liang, B. CO₂ Capture from Flue Gas Using an Electrochemically Reversible Hydroquinone/Quinone Solution. *Energy Fuels* **2019**, 33 (4), 3380–3389.
- (19) Xie, H.; Wu, Y.; Liu, T.; Wang, F.; Chen, B.; Liang, B. Low-energy-consumption electrochemical CO₂ capture driven by biomimetic phenazine derivatives redox medium. *Appl. Energy* **2020**, 259, No. 114119.
- (20) Rahimi, M.; Catalini, G.; Hariharan, S.; Wang, M.; Puccini, M.; Hatton, T. A. Carbon Dioxide Capture Using an Electrochemically Driven Proton Concentration Process. *Cell Rep. Phys. Sci.* **2020**, 1 (4), No. 100033.
- (21) Jin, S.; Wu, M.; Gordon, R. G.; Aziz, M. J.; Kwabi, D. G. pH swing cycle for CO₂ capture electrochemically driven through proton-coupled electron transfer. *Energy Environ. Sci.* **2020**, 13 (10), 3706–3722.
- (22) Seo, H.; Hatton, T. A. Electrochemical direct air capture of CO₂ using neutral red as reversible redox-active material. *Nat. Commun.* **2023**, 14 (1), No. 313.
- (23) Kim, S.; Nitzsche, M. P.; Rufer, S. B.; Lake, J. R.; Varanasi, K. K.; Hatton, T. A. Asymmetric chloride-mediated electrochemical process for CO₂ removal from oceanwater. *Energy Environ. Sci.* **2023**, 16 (5), 2030–2044.
- (24) Apaydin, D. H.; Glowacki, E. D.; Portenkirchner, E.; Sariciftci, N. S. Direct Electrochemical Capture and Release of Carbon Dioxide Using an Industrial Organic Pigment: Quinacridone. *Angew. Chem., Int. Ed.* **2014**, 53 (26), 6819–6822.
- (25) Ranjan, R.; Olson, J.; Singh, P.; Lorange, E. D.; Buttry, D. A.; Gould, I. R. Reversible Electrochemical Trapping of Carbon Dioxide Using 4,4'-Bipyridine That Does Not Require Thermal Activation. *J. Phys. Chem. Lett.* **2015**, 6 (24), 4943–4946.
- (26) Singh, P.; Rheinhardt, J. H.; Olson, J. Z.; Tarakeshwar, P.; Mujica, V.; Buttry, D. A. Electrochemical Capture and Release of Carbon Dioxide Using a Disulfide–Thiocarbonate Redox Cycle. *J. Am. Chem. Soc.* **2017**, 139 (3), 1033–1036.
- (27) Seo, H.; Rahimi, M.; Hatton, T. A. Electrochemical Carbon Dioxide Capture and Release with a Redox-Active Amine. *J. Am. Chem. Soc.* **2022**, 144 (5), 2164–2170.
- (28) Li, X.; Zhao, X.; Liu, Y.; Hatton, T. A.; Liu, Y. Redox-tunable Lewis bases for electrochemical carbon dioxide capture. *Nat. Energy* **2022**, 7 (11), 1065–1075.
- (29) Rheinhardt, J. H.; Singh, P.; Tarakeshwar, P.; Buttry, D. A. Electrochemical Capture and Release of Carbon Dioxide. *ACS Energy Lett.* **2017**, 2 (2), 454–461.
- (30) Muroyama, A. P.; Pătru, A.; Gubler, L. Review—CO₂ Separation and Transport via Electrochemical Methods. *J. Electrochem. Soc.* **2020**, 167 (13), No. 133504.
- (31) Renfrew, S. E.; Starr, D. E.; Strasser, P. Electrochemical Approaches toward CO₂ Capture and Concentration. *ACS Catal.* **2020**, 10 (21), 13058–13074.
- (32) Sharifian, R.; Wagterveld, R. M.; Digdaya, I. A.; Xiang, C.; Vermaas, D. A. Electrochemical carbon dioxide capture to close the carbon cycle. *Energy Environ. Sci.* **2021**, 14 (2), 781–814.
- (33) Kang, J. S.; Kim, S.; Hatton, T. A. Redox-responsive sorbents and mediators for electrochemically based CO₂ capture. *Curr. Opin. Green Sustainable Chem.* **2021**, 31, No. 100504.
- (34) Diederichsen, K. M.; Sharifian, R.; Kang, J. S.; Liu, Y.; Kim, S.; Gallant, B. M.; Vermaas, D.; Hatton, T. A. Electrochemical methods for carbon dioxide separations. *Nat. Rev. Methods Primers* **2022**, 2 (1), 68.
- (35) Rahimi, M.; Khurram, A.; Hatton, T. A.; Gallant, B. Electrochemical carbon capture processes for mitigation of CO₂ emissions. *Chem. Soc. Rev.* **2022**, 51 (20), 8676–8695.
- (36) Li, X.; Mathur, A.; Liu, A.; Liu, Y. Electrifying Carbon Capture by Developing Nanomaterials at the Interface of Molecular and Process Engineering. *Acc. Chem. Res.* **2023**, 56 (20), 2763–2775.
- (37) Seo, H.; Nitzsche, M. P.; Hatton, T. A. Redox-Mediated pH Swing Systems for Electrochemical Carbon Capture. *Acc. Chem. Res.* **2023**, 56 (22), 3153–3164.
- (38) Massen-Hane, M.; Diederichsen, K. M.; Hatton, T. A. Engineering redox-active electrochemically mediated carbon dioxide capture systems. *Nat. Chem. Eng.* **2024**, 1 (1), 35–44.
- (39) Radjenovic, J.; Sedlak, D. L. Challenges and Opportunities for Electrochemical Processes as Next-Generation Technologies for the Treatment of Contaminated Water. *Environ. Sci. Technol.* **2015**, 49 (19), 11292–11302.
- (40) Su, X.; Hatton, T. A. Redox-electrodes for selective electrochemical separations. *Adv. Colloid Interface Sci.* **2017**, 244, 6–20.
- (41) Chaplin, B. P. The Prospect of Electrochemical Technologies Advancing Worldwide Water Treatment. *Acc. Chem. Res.* **2019**, 52 (3), 596–604.
- (42) Tan, K.-J.; Hatton, T. A. Electrochemically Mediated Sustainable Separations in Water. In *Sustainable Separation Engineering*; John Wiley & Sons Ltd., 2022; pp 1–62.
- (43) Bell, W. L.; Miedaner, A.; Smart, J. C.; DuBois, D. L.; Verostko, C. E. Synthesis and Evaluation of Electroactive CO₂ Carriers. *SAE Trans.* **1988**, 97, 544–552.
- (44) De Sousa Bulhões, L. O.; Zara, A. J. The effect of carbon dioxide on the electroreduction of 1,4-benzoquinone. *J. Electroanal. Chem. Interfacial Electrochem.* **1988**, 248 (1), 159–165.
- (45) Mizen, M. B.; Wrighton, M. S. Reductive Addition of CO₂ to 9,10-Phenanthrenequinone. *J. Electrochem. Soc.* **1989**, 136 (4), 941.
- (46) Comeau Simpson, T.; Durand, R. R. Reactivity of carbon dioxide with quinones. *Electrochim. Acta* **1990**, 35 (9), 1399–1403.
- (47) DuBois, D. L.; Miedaner, A.; Bell, W.; Smart, J. C. Electrochemical Concentration of Carbon Dioxide. In *Electrochemical and Electrocatalytic Reactions of Carbon Dioxide*; Sullivan, B. P.; Krist, K.; Guard, H. E., Eds.; Elsevier Science, 1993; pp 94–117.
- (48) Scovazzo, P.; Poshusta, J.; DuBois, D.; Koval, C.; Noble, R. Electrochemical Separation and Concentration of <1% Carbon Dioxide from Nitrogen. *J. Electrochem. Soc.* **2003**, 150 (5), D91.
- (49) Gurkan, B.; Simeon, F.; Hatton, T. A. Quinone Reduction in Ionic Liquids for Electrochemical CO₂ Separation. *ACS Sustainable Chem. Eng.* **2015**, 3 (7), 1394–1405.
- (50) Voskian, S.; Hatton, T. A. Faradaic electro-swing reactive adsorption for CO₂ capture. *Energy Environ. Sci.* **2019**, 12 (12), 3530–3547.
- (51) Liu, Y.; Ye, H.-Z.; Diederichsen, K. M.; Van Voorhis, T.; Hatton, T. A. Electrochemically mediated carbon dioxide separation with quinone chemistry in salt-concentrated aqueous media. *Nat. Commun.* **2020**, 11 (1), No. 2278.
- (52) Liu, Y.; Chow, C.-M.; Phillips, K. R.; Wang, M.; Voskian, S.; Hatton, T. A. Electrochemically mediated gating membrane with dynamically controllable gas transport. *Sci. Adv.* **2020**, 6 (42), No. eabc1741.
- (53) Tam, S. M.; Tessensohn, M. E.; Tan, J. Y.; Subrata, A.; Webster, R. D. Competition between Reversible Capture of CO₂ and Release of CO₂•– Using Electrochemically Reduced Quinones in Acetonitrile Solutions. *J. Phys. Chem. C* **2021**, 125 (22), 11916–11927.
- (54) Diederichsen, K. M.; Liu, Y.; Ozbek, N.; Seo, H.; Hatton, T. A. Toward solvent-free continuous-flow electrochemically mediated carbon capture with high-concentration liquid quinone chemistry. *Joule* **2022**, 6 (1), 221–239.
- (55) Hemmatifar, A.; Kang, J. S.; Ozbek, N.; Tan, K.-J.; Hatton, T. A. Electrochemically Mediated Direct CO₂ Capture by a Stackable Bipolar Cell. *ChemSusChem* **2022**, 15 (6), No. e202102533.
- (56) Diederichsen, K. M.; DeWitt, S. J. A.; Hatton, T. A. Electrochemically Facilitated Transport of CO₂ between Gas Diffusion Electrodes in Flat and Hollow Fiber Geometries. *ACS ES&T Eng.* **2023**, 3 (7), 1001–1012.

- (57) Simeon, F.; Stern, M. C.; Diederichsen, K. M.; Liu, Y.; Herzog, H. J.; Hatton, T. A. Electrochemical and Molecular Assessment of Quinones as CO₂-Binding Redox Molecules for Carbon Capture. *J. Phys. Chem. C* **2022**, *126* (3), 1389–1399.
- (58) Barlow, J. M.; Yang, J. Y. Oxygen-Stable Electrochemical CO₂ Capture and Concentration with Quinones Using Alcohol Additives. *J. Am. Chem. Soc.* **2022**, *144* (31), 14161–14169.
- (59) Bui, A. T.; Hartley, N. A.; Thom, A. J. W.; Forse, A. C. Trade-Off between Redox Potential and the Strength of Electrochemical CO₂ Capture in Quinones. *J. Phys. Chem. C* **2022**, *126* (33), 14163–14172.
- (60) Schimanofsky, C.; Wielend, D.; Kröll, S.; Lerch, S.; Werner, D.; Gallmetzer, J. M.; Mayr, F.; Neugebauer, H.; Irimia-Vladu, M.; Portenkirchner, E.; et al. Direct Electrochemical CO₂ Capture Using Substituted Anthraquinones in Homogeneous Solutions: A Joint Experimental and Theoretical Study. *J. Phys. Chem. C* **2022**, *126* (33), 14138–14154.
- (61) Zito, A. M.; Bím, D.; Vargas, S.; Alexandrova, A. N.; Yang, J. Y. Computational and Experimental Design of Quinones for Electrochemical CO₂ Capture and Concentration. *ACS Sustainable Chem. Eng.* **2022**, *10* (34), 11387–11395.
- (62) Xu, Y.; Zheng, M.; Musgrave, C. B., III; Zhang, L.; Goddard, W. A., III; Bukowski, B. C.; Liu, Y. Assessing the Kinetics of Quinone–CO₂ Adduct Formation for Electrochemically Mediated Carbon Capture. *ACS Sustainable Chem. Eng.* **2023**, *11* (30), 11333–11341.
- (63) Nohl, H.; Jordan, W.; Youngman, R. J. Quinones in Biology: Functions in electron transfer and oxygen activation. *Adv. Free Radical Biol. Med.* **1986**, *2* (1), 211–279.
- (64) Mladěnka, P.; Macáková, K.; Kujovská Krčmová, L.; Javorská, L.; Mrštná, K.; Carazo, A.; Protti, M.; Remião, F.; Nováková, L. Vitamin K – sources, physiological role, kinetics, deficiency, detection, therapeutic use, and toxicity. *Nutr. Rev.* **2022**, *80* (4), 677–698.
- (65) Turunen, M.; Olsson, J.; Dallner, G. Metabolism and function of coenzyme Q. *Biochim. Biophys. Acta* **2004**, *1660* (1), 171–199.
- (66) Lovander, M. D.; Lyon, J. D.; Parr, D. L.; Wang, J.; Parke, B.; Leddy, J. Critical Review—Electrochemical Properties of 13 Vitamins: A Critical Review and Assessment. *J. Electrochem. Soc.* **2018**, *165* (2), G18.
- (67) Gulaboski, R.; Markovski, V.; Jihe, Z. Redox chemistry of coenzyme Q—a short overview of the voltammetric features. *J. Solid State Electrochem.* **2016**, *20* (12), 3229–3238.
- (68) Trumpower, B. L. *Function of Quinones in Energy Conserving Systems*; Academic Press, 1982.
- (69) Olson, R. E. The Function and Metabolism of Vitamin K. *Annu. Rev. Nutr.* **1984**, *4* (1), 281–337.
- (70) Crane, F. L.; Navas, P. The diversity of coenzyme Q function. *Mol. Asp. Med.* **1997**, *18*, 1–6.
- (71) Stafford, D. W. The vitamin K cycle. *J. Thromb. Haemostasis* **2005**, *3* (8), 1873–1878.
- (72) Brandt, U.; Trumpower, B. The Protonmotive Q Cycle in Mitochondria and Bacteria. *Crit. Rev. Biochem. Mol. Biol.* **1994**, *29* (3), 165–197.
- (73) Wang, H.; Yang, Y.; Guo, L. Nature-Inspired Electrochemical Energy-Storage Materials and Devices. *Adv. Energy Mater.* **2017**, *7* (5), No. 1601709.
- (74) Sato, F.; Togo, M.; Islam, M. K.; Matsue, T.; Kosuge, J.; Fukasaku, N.; Kurosawa, S.; Nishizawa, M. Enzyme-based glucose fuel cell using Vitamin K3-immobilized polymer as an electron mediator. *Electrochem. Commun.* **2005**, *7* (7), 643–647.
- (75) Zhang, Y.; Wang, L.; Zhang, X.; Guo, L.; Wang, Y.; Peng, Z. High-Capacity and High-Rate Discharging of a Coenzyme Q10-Catalyzed Li–O₂ Battery. *Adv. Mater.* **2018**, *30* (5), No. 1705571.
- (76) Xue, Q.; Li, D.; Huang, Y.; Zhang, X.; Ye, Y.; Fan, E.; Li, L.; Wu, F.; Chen, R. Vitamin K as a high-performance organic anode material for rechargeable potassium ion batteries. *J. Mater. Chem. A* **2018**, *6* (26), 12559–12564.
- (77) Mårtensson, C.; Agmo Hernández, V. Ubiquinone-10 in gold-immobilized lipid membrane structures acts as a sensor for acetylcholine and other tetraalkylammonium cations. *Bioelectrochemistry* **2012**, *88*, 171–180.
- (78) Ru, J.; Du, J.; Qin, D.-D.; Huang, B.-M.; Xue, Z.-H.; Zhou, X.-B.; Lu, X.-Q. An electrochemical glutathione biosensor: Ubiquinone as a transducer. *Talanta* **2013**, *110*, 15–20.
- (79) McBeth, C.; Dughaishi, R. A.; Paterson, A.; Sharp, D. Ubiquinone modified printed carbon electrodes for cell culture pH monitoring. *Biosens. Bioelectron.* **2018**, *113*, 46–51.
- (80) Brunmark, A.; Cadenas, E. Redox and addition chemistry of quinoid compounds and its biological implications. *Free Radical Biol. Med.* **1989**, *7* (4), 435–477.
- (81) Tan, K.-J.; Su, X.; Hatton, T. A. An Asymmetric Iron-Based Redox-Active System for Electrochemical Separation of Ions in Aqueous Media. *Adv. Funct. Mater.* **2020**, *30* (15), No. 1910363.
- (82) Tan, K.-J.; Morikawa, S.; Phillips, K. R.; Ozbek, N.; Hatton, T. A. Redox-Active Magnetic Composites for Anionic Contaminant Removal from Water. *ACS Appl. Mater. Interfaces* **2022**, *14* (7), 8974–8983.
- (83) Tan, K.-J.; Morikawa, S.; Ozbek, N.; Lenz, M.; Arlt, C.-R.; Tschöpe, A.; Franzreb, M.; Hatton, T. A. Redox Polyelectrolytes with pH-Sensitive Electroactive Functionality in Aqueous Media. *Langmuir* **2023**, *39* (8), 2943–2956.
- (84) Tan, K.-J.; Morikawa, S.; Hemmatifar, A.; Ozbek, N.; Liu, Y.; Hatton, T. A. Hydrophobicity Tuned Polymeric Redox Materials with Solution-Specific Electroactive Properties for Selective Electrochemical Metal Ion Recovery in Aqueous Environments. *ACS Appl. Mater. Interfaces* **2023**, *15* (37), 43859–43870.
- (85) Tan, K.-J.; Morikawa, S.; Hatton, T. A. Electroactive Behavior of Adjustable Vinylferrocene Copolymers in Electrolyte Media. *J. Phys. Chem. B* **2024**, *128* (7), 1748–1759.
- (86) Su, X.; Bromberg, L.; Tan, K.-J.; Jamison, T. F.; Padhye, L. P.; Hatton, T. A. Electrochemically Mediated Reduction of Nitrosamines by Hemin-Functionalized Redox Electrodes. *Environ. Sci. Technol. Lett.* **2017**, *4* (4), 161–167.
- (87) Bromberg, L.; Ozbek, N.; Tan, K.-J.; Su, X.; Padhye, L. P.; Alan Hatton, T. Iron phosphomolybdate complexes in electrocatalytic reduction of aqueous disinfection byproducts. *Chem. Eng. J.* **2021**, *408*, No. 127354.
- (88) Hansen, C. M. *The Three Dimensional Solubility Parameter And Solvent Diffusion Coefficient*; Danish Technical Press: Copenhagen, 1967.
- (89) Hansen, C. M. Determination of Hansen Solubility Parameter Values for Carbon Dioxide. In *Hansen Solubility Parameters: A User's Handbook*, 2nd ed.; CRC Press, 2007; p 177.
- (90) Hansen, C. M. Solubility Parameters – An Introduction. In *Hansen Solubility Parameters: A User's Handbook*, 2nd ed.; CRC Press, 2007; p 7.
- (91) Cumming, H.; Rücker, C. Octanol–Water Partition Coefficient Measurement by a Simple ¹H NMR Method. *ACS Omega* **2017**, *2* (9), 6244–6249.
- (92) Hansch, C.; Leo, A. *Substituent Constants for Correlation Analysis in Chemistry and Biology*; Wiley, 1979.
- (93) Viswanadhan, V. N.; Ghose, A. K.; Revankar, G. R.; Robins, R. K. Atomic physicochemical parameters for three dimensional structure directed quantitative structure-activity relationships. 4. Additional parameters for hydrophobic and dispersive interactions and their application for an automated superposition of certain naturally occurring nucleoside antibiotics. *J. Chem. Inf. Comput. Sci.* **1989**, *29* (3), 163–172.
- (94) Moriguchi, I.; Hirono, S.; Liu, Q.; Nakagome, I.; Matsushita, Y. Simple Method of Calculating Octanol/Water Partition Coefficient. *Chem. Pharm. Bull.* **1992**, *40* (1), 127–130.
- (95) Moriguchi, I.; Hirono, S.; Nakagome, I.; Hirano, H. Comparison of Reliability of log P Values for Drugs Calculated by Several Methods. *Chem. Pharm. Bull.* **1994**, *42* (4), 976–978.
- (96) Jemiot-Rzemińska, M.; Latowski, D.; Strzałka, K. Incorporation of plastoquinone and ubiquinone into liposome membranes

studied by HPLC analysis.: The effect of side chain length and redox state of quinone. *Chem. Phys. Lipids* **2001**, *110* (1), 85–94.

(97) Suhara, Y.; Kamao, M.; Tsugawa, N.; Okano, T. Method for the Determination of Vitamin K Homologues in Human Plasma Using High-Performance Liquid Chromatography-Tandem Mass Spectrometry. *Anal. Chem.* **2005**, *77* (3), 757–763.

(98) Korsten, H. Viscosity of liquid hydrocarbons and their mixtures. *AIChE J.* **2001**, *47* (2), 453–462.

(99) Dobrynin, A. V.; Sayko, R.; Colby, R. H. Viscosity of Polymer Solutions and Molecular Weight Characterization. *ACS Macro Lett.* **2023**, *12* (6), 773–779.

(100) Quan, M.; Sanchez, D.; Wasylkiw, M. F.; Smith, D. K. Voltammetry of Quinones in Unbuffered Aqueous Solution: Reassessing the Roles of Proton Transfer and Hydrogen Bonding in the Aqueous Electrochemistry of Quinones. *J. Am. Chem. Soc.* **2007**, *129* (42), 12847–12856.

(101) Gupta, N.; Linschitz, H. Hydrogen-Bonding and Protonation Effects in Electrochemistry of Quinones in Aprotic Solvents. *J. Am. Chem. Soc.* **1997**, *119* (27), 6384–6391.

(102) Hui, Y.; Chng, E. L. K.; Chng, C. Y. L.; Poh, H. L.; Webster, R. D. Hydrogen-Bonding Interactions between Water and the One- and Two-Electron-Reduced Forms of Vitamin K1: Applying Quinone Electrochemistry To Determine the Moisture Content of Non-Aqueous Solvents. *J. Am. Chem. Soc.* **2009**, *131* (4), 1523–1534.

(103) Staley, R. P.-A.; Lopez, E. M.; Clare, L. A.; Smith, D. K. Kinetic Stabilization of Quinone Dianions via Hydrogen Bonding by Water in Aprotic Solvents. *J. Phys. Chem. C* **2015**, *119* (35), 20319–20327.

(104) Yin, W.; Grimaud, A.; Azcarate, I.; Yang, C.; Tarascon, J.-M. Electrochemical Reduction of CO₂ Mediated by Quinone Derivatives: Implication for Li–CO₂ Battery. *J. Phys. Chem. C* **2018**, *122* (12), 6546–6554.

(105) Nagaoka, T.; Nishii, N.; Fujii, K.; Ogura, K. Mechanisms of reductive addition of CO₂ to quinones in acetonitrile. *J. Electroanal. Chem.* **1992**, *322* (1), 383–389.

(106) Namazian, M.; Zare, H. R.; Yousofian-Varzaneh, H. Electrochemical behavior of tetrafluoro-p-benzoquinone at the presence of carbon dioxide: Experimental and theoretical studies. *Electrochim. Acta* **2016**, *196*, 692–698.

(107) Vasudevan, D.; Wendt, H. Electroreduction of oxygen in aprotic media. *J. Electroanal. Chem.* **1995**, *392* (1), 69–74.

(108) Petrucci, R.; Giorgini, E.; Damiani, E.; Carloni, P.; Marrosu, G.; Trazza, A.; Littarru, G. P.; Greci, L. A study on the interactions between coenzyme Q₀ and superoxide anion. Could ubiquinones mimic superoxide dismutase (SOD)? *Res. Chem. Intermed.* **2000**, *26* (3), 269–282.

(109) Samoilova, R. I.; Crofts, A. R.; Dikanov, S. A. Reaction of Superoxide Radical with Quinone Molecules. *J. Phys. Chem. A* **2011**, *115* (42), 11589–11593.

(110) Roberts, J. L., Jr.; Calderwood, T. S.; Sawyer, D. T. Nucleophilic oxygenation of carbon dioxide by superoxide ion in aprotic media to form the peroxydicarbonate(2-) ion species. *J. Am. Chem. Soc.* **1984**, *106* (17), 4667–4670.

(111) Wadhawan, J. D.; Welford, P. J.; Maisonhaute, E.; Climent, V.; Lawrence, N. S.; Compton, R. G.; McPeak, H. B.; Hahn, C. E. W. Microelectrode Studies of the Reaction of Superoxide with Carbon Dioxide in Dimethyl Sulfoxide. *J. Phys. Chem. B* **2001**, *105* (43), 10659–10668.

(112) Elgrishi, N.; Rountree, K. J.; McCarthy, B. D.; Rountree, E. S.; Eisenhart, T. T.; Dempsey, J. L. A Practical Beginner's Guide to Cyclic Voltammetry. *J. Chem. Educ.* **2018**, *95* (2), 197–206.

(113) Hansch, C.; Leo, A.; Taft, R. W. A survey of Hammett substituent constants and resonance and field parameters. *Chem. Rev.* **1991**, *91* (2), 165–195.

(114) Prince, R. C.; Dutton, P. L.; Bruce, J. M. Electrochemistry of ubiquinones: Menaquinones and plastoquinones in aprotic solvents. *FEBS Lett.* **1983**, *160* (1), 273–276.

(115) Bauscher, M.; Maentele, W. Electrochemical and infrared-spectroscopic characterization of redox reactions of p-quinones. *J. Phys. Chem.* **1992**, *96* (26), 11101–11108.

(116) Nasiri, H. R.; Panisch, R.; Madej, M. G.; Bats, J. W.; Lancaster, C. R. D.; Schwalbe, H. The correlation of cathodic peak potentials of vitamin K3 derivatives and their calculated electron affinities: The role of hydrogen bonding and conformational changes. *Biochim. Biophys. Acta* **2009**, *1787* (6), 601–608.

(117) Ma, W.; Zhou, H.; Ying, Y.-L.; Li, D.-W.; Chen, G.-R.; Long, Y.-T.; Chen, H.-Y. In situ spectroelectrochemistry and cytotoxic activities of natural ubiquinone analogues. *Tetrahedron* **2011**, *67* (33), 5990–6000.

(118) El-Hout, S. I.; Suzuki, H.; El-Sheikh, S. M.; Hassan, H. M. A.; Harraz, F. A.; Ibrahim, I. A.; El-Sharkawy, E. A.; Tsujimura, S.; Holzinger, M.; Nishina, Y. Tuning the redox potential of vitamin K3 derivatives by oxidative functionalization using a Ag(i)/GO catalyst. *Chem. Commun.* **2017**, *53* (63), 8890–8893.

(119) Prince, R. C.; Dutton, P. L.; Gunner, M. R. The aprotic electrochemistry of quinones. *Biochim. Biophys. Acta* **2022**, *1863* (6), No. 148558.

(120) Prince, R. C.; Halbert, T. R.; Upton, T. H. Structural Influences on the Electrochemistry of Ubiquinone. In *Advances in Membrane Biochemistry and Bioenergetics*; Kim, C. H.; Tedeschi, H.; Diwan, J. J.; Salerno, J. C., Eds.; Springer US, 1987; pp 469–478.

(121) Burie, J.-R.; Boullais, C.; Nonella, M.; Mioskowski, C.; Nabadryk, E.; Breton, J. Importance of the Conformation of Methoxy Groups on the Vibrational and Electrochemical Properties of Ubiquinones. *J. Phys. Chem. B* **1997**, *101* (33), 6607–6617.

(122) Yu, C.; Gu, L.; Lin, Y.; Yu, L. Effect of alkyl side chain variation on the electron-transfer activity of ubiquinone derivatives. *Biochemistry* **1985**, *24* (15), 3897–3902.

(123) Rowe, G. K.; Creager, S. E. Redox and ion-pairing thermodynamics in self-assembled monolayers. *Langmuir* **1991**, *7* (10), 2307–2312.

(124) Rowe, G. K.; Creager, S. E. Interfacial Solvation and Double-Layer Effects on Redox Reactions in Organized Assemblies. *J. Phys. Chem.* **1994**, *98* (21), 5500–5507.

(125) Batchelor-McAuley, C.; Li, Q.; Dapin, S. M.; Compton, R. G. Voltammetric Characterization of DNA Intercalators across the Full pH Range: Anthraquinone-2,6-disulfonate and Anthraquinone-2-sulfonate. *J. Phys. Chem. B* **2010**, *114* (11), 4094–4100.

(126) Wilhelmsen, C. O.; Kristensen, S. B.; Nolte, O.; Volodin, I. A.; Christiansen, J. V.; Isbrandt, T.; Sørensen, T.; Petersen, C.; Sondergaard, T. E.; Lehmann Nielsen, K.; et al. Demonstrating the Use of a Fungal Synthesized Quinone in a Redox Flow Battery. *Batteries Supercaps* **2023**, *6* (1), No. e202200365.

(127) Bard, A. J.; Faulkner, L. R. *Electrochemical Methods: Fundamentals and Applications*, 2nd ed.; John Wiley & Sons, Inc., 2000.

(128) Shen, X.; Sinclair, N.; Wainright, J.; Imel, A.; Barth, B.; Zawodzinski, T.; Savinell, R. F. A Study of Ferrocene Diffusion in Toluene/Tween 20/1-Butanol/Water Microemulsions for Redox Flow Battery Applications. *J. Electrochem. Soc.* **2021**, *168* (6), No. 060539.

(129) Ding, Y.; Li, Y.; Yu, G. Exploring Bio-inspired Quinone-Based Organic Redox Flow Batteries: A Combined Experimental and Computational Study. *Chem* **2016**, *1* (5), 790–801.

(130) Lenaz, G.; Fato, R.; Formiggini, G.; Genova, M. L. The role of Coenzyme Q in mitochondrial electron transport. *Mitochondrion* **2007**, *7*, S8–S33.

(131) Zu, Y.; Shannon, R. J.; Hirst, J. Reversible, Electrochemical Interconversion of NADH and NAD⁺ by the Catalytic (I_L) Subcomplex of Mitochondrial NADH:Ubiquinone Oxidoreductase (Complex I). *J. Am. Chem. Soc.* **2003**, *125* (20), 6020–6021.

(132) Ma, W.; Li, D.-W.; Sutherland, T. C.; Li, Y.; Long, Y.-T.; Chen, H.-Y. Reversible Redox of NADH and NAD⁺ at a Hybrid Lipid Bilayer Membrane Using Ubiquinone. *J. Am. Chem. Soc.* **2011**, *133* (32), 12366–12369.

- (133) Haynes, W. M. *CRC Handbook of Chemistry and Physics*, 91st ed.; Taylor & Francis Group, 2010.
- (134) Zhou, F.; Hearne, Z.; Li, C.-J. Water—the greenest solvent overall. *Curr. Opin. Green Sustainable Chem.* **2019**, *18*, 118–123.
- (135) Moret, V.; Pinamonti, S.; Fornasari, E. Polarographic study on the redox potential of ubiquinones. *Biochim. Biophys. Acta* **1961**, *54* (2), 381–383.
- (136) Ksenzhek, O. S.; Petrova, S. A.; Kolodyazhny, M. V. 452 — Redox properties of ubiquinones in aqueous solutions. *Bioelectrochem. Bioenerg.* **1982**, *9* (2), 167–174.
- (137) Petrova, S. A.; Ksenzhek, O. S.; Koiodyazhnyi, M. V. Redox properties of naturally occurring naphthoquinones: Vitamin K₂(20) and lapachol. *Russ. J. Electrochem.* **2000**, *36* (7), 767–772.
- (138) Wain, A. J.; Wadhawan, J. D.; Compton, R. G. Electrochemical Studies of Vitamin K₁ Microdroplets: Electrocatalytic Hydrogen Evolution. *ChemPhysChem* **2003**, *4* (9), 974–982.
- (139) Gulaboski, R.; Bogeski, I.; Kokoskarova, P.; Haeri, H. H.; Mitrev, S.; Stefova, M.; Stanoeva, J. P.; Markovski, V.; Mirceski, V.; Hoth, M.; Kappl, R. New insights into the chemistry of Coenzyme Q₀: A voltammetric and spectroscopic study. *Bioelectrochemistry* **2016**, *111*, 100–108.
- (140) Hua, X.; Xia, H.-L.; Ying, Y.-L.; Long, Y.-T. Proton-Coupled Electron Transfer of Coenzyme Q in Unbuffered Solution by Pore Confined In Situ Liquid ToF-SIMS. *J. Electrochem. Soc.* **2022**, *169* (2), No. 026525.
- (141) Bunpheng, A.; Sakulaue, P.; Hirunpinyopas, W.; Nueangnoraj, K.; Luanwuthi, S.; Iamprasertkun, P. Revisiting the properties of lithium chloride as “water-in-salt” electrolyte for pouch cell electrochemical capacitors. *J. Electroanal. Chem.* **2023**, *944*, No. 117645.
- (142) Suo, L.; Borodin, O.; Gao, T.; Olguin, M.; Ho, J.; Fan, X.; Luo, C.; Wang, C.; Xu, K. Water-in-salt” electrolyte enables high-voltage aqueous lithium-ion chemistries. *Science* **2015**, *350* (6263), 938–943.
- (143) Takehara, K.; Ide, Y. Electrochemical behaviour of the ubiquinone-Q₁₀ film coated onto a glassy carbon electrode by the spinner method. *J. Electroanal. Chem. Interfacial Electrochem.* **1991**, *321* (2), 297–305.
- (144) Gordillo, G. J.; Schiffrin, D. J. Redox properties of ubiquinone (UQ₁₀) adsorbed on a mercury electrode. *J. Chem. Soc., Faraday Trans.* **1994**, *90* (13), 1913–1922.
- (145) Bilewicz, R.; Majda, M. Monomolecular Langmuir-Blodgett films at electrodes. Formation of passivating monolayers and incorporation of electroactive reagents. *Langmuir* **1991**, *7* (11), 2794–2802.
- (146) Moncelli, M. R.; Herrero, R.; Becucci, L.; Guidelli, R. Kinetics of electron and proton transfer to ubiquinone-10 and from ubiquinol-10 in a self-assembled phosphatidylcholine monolayer. *Biochim. Biophys. Acta* **1998**, *1364* (3), 373–384.
- (147) Gordillo, G. J.; Schiffrin, D. J. The electrochemistry of ubiquinone-10 in a phospholipid model membrane. *Faraday Discuss.* **2000**, *116* (0), 89–107.
- (148) Hoyo, J.; Gaus, E.; Oncins, G.; Torrent-Burgués, J.; Sanz, F. Incorporation of Ubiquinone in Supported Lipid Bilayers on ITO. *J. Phys. Chem. B* **2013**, *117* (25), 7498–7506.
- (149) Lawrence, K.; Watkins, J. D.; James, T. D.; Taylor, J. E.; Bull, S. D.; Nelson, G. W.; Foord, J. S.; Long, Y.-T.; Marken, F. Dioctylamine-Sulfonamide-Modified Carbon Nanoparticles as High Surface Area Substrates for Coenzyme Q₁₀-Lipid Electrochemistry. *Electroanalysis* **2012**, *24* (5), 1003–1010.
- (150) Arthisree, D.; Devi, K. S. S.; Devi, S. L.; Meera, K.; Joshi, G. M.; Senthil Kumar, A. A hydrophobic coenzyme Q₁₀ stabilized functionalized-MWCNT modified electrode as an efficient functional biomimetic system for the electron-transfer study. *Colloids Surf., A* **2016**, *504*, 53–61.